Liquid Crystals
Publication details, including instructions for authors and subscription information:
http://www.informaworld.com/smpp/title~content=t713926090

Anomalous thermal hysteresis in the SmC* phase of 10FHBBBM7*, revealed by dielectric measurements

S. Sarmento; P. Simeão Carvalho; M. R. Chaves; F. Pinto; H. T. Nguyen

Online publication date: 06 August 2010

To cite this Article Sarmento, S. , Carvalho, P. Simeão , Chaves, M. R. , Pinto, F. and Nguyen, H. T.(2001) 'Anomalous thermal hysteresis in the SmC* phase of 10FHBBBM7*, revealed by dielectric measurements', Liquid Crystals, 28: 12, 1839 — 1845
To link to this Article: DOI: 10.1080/02678290110086532
URL: http://dx.doi.org/10.1080/02678290110086532

LIQUID CRYSTALS, 2001, VOL. 28, NO. 12, 1839–1845

Anomalous thermal hysteresis in the SmC* phase of 10FHBBBM7*, revealed by dielectric measurements

S. SARMENTO, P. SIMEÃO CARVALHO, M. R. CHAVES*, F. PINTO
Departamento de Física, IFIMUP, CFUP,
Faculdade de Ciências da Universidade do Porto, Rua do Campo Alegre 687,
4169-007 Porto, Portugal

and H. T. NGUYEN
Centre de Recherche Paul Pascal, Av. A. Schweitzer, 33600 Pessac, France

(*Received 21 October 2000; accepted 18 June 2001*)

The SmC* phase of (*R*)-4-(1-methylheptyloxycarbonyl)phenyl 4′-(4-decyloxy-3-fluorobenzoyloxy)-benzoate, 10FHBBBM7*, shows an anomalous thermal hysteresis that is reflected in the values of the measured dielectric constant. When the cooling–heating cycle is repeated, a memory effect occurs. In this work, we present a detailed study and a tentative interpretation of this unusual effect.

1. Introduction

In a previous study [1], we reported a detailed dielectric study of three chiral liquid crystals which exhibit ferrielectric phases over large temperature ranges. For one of these compounds, 10FHBBBM7* or simple 10FH, we found a very different value of the dielectric constant in the SmC* phase, on cooling and on heating runs. The relevant aspects of this anomalous thermal hysteresis are presented here and examined in detail.

The compound 10FH has the chemical structure [2]:

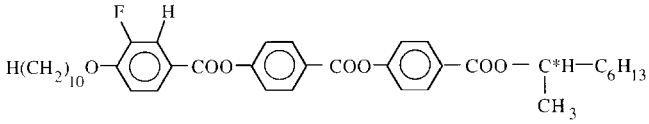

and shows the phase sequence:

$$\mathrm{Cr–SmC^*_A–SmC^*_{FI}–SmC^*–SmC^*_\alpha–SmA^*–I}$$

The transition temperatures determined [1] on heating ($\rightharpoonup$) and cooling ($\leftharpoondown$) are:

$$\mathrm{SmC^*_A} \underset{101.9}{\overset{103.1}{\rightleftharpoons}} \mathrm{SmC^*_{FI}} \underset{104.0}{\overset{105.1}{\rightleftharpoons}} \mathrm{SmC^*} \underset{113.8}{\overset{113.8}{\rightleftharpoons}}$$

$$\mathrm{SmC^*_\alpha} \underset{114.7}{\overset{114.7}{\rightleftharpoons}} \mathrm{SmA^*}\ (^\circ\mathrm{C})$$

2. Experimental

Commercial cells (EHC Co., Japan), coated with ITO electrodes and rubbed polyimide, were filled by capillary action with the liquid crystals. All measurements were made on planar, 25 μm thick samples. To ensure the best possible alignment, the samples were cooled slowly ($0.25^\circ\mathrm{C\ min^{-1}}$) from the isotropic phase and an a.c. electric field (10–50 Hz, 0.8–1.0 $\mathrm{V\ \mu m^{-1}}$) was applied just below the temperature of the $\mathrm{SmC^*_\alpha}$–SmA* phase transition for 20–30 min before each measurement.

The samples were placed in a purpose built oven and the temperature was controlled with a Lakeshore DRC-93CA temperature controller, using a chromel alumel thermocouple. The accuracy was about 0.05 K.

The dielectric constant was measured at stabilized temperatures on cooling and heating, in the frequency range 20 Hz–1 MHz, using a HP4284A LCR meter and a measuring electric field of 0.01 $\mathrm{V\ \mu m^{-1}}$. The resistance of the electrodes in series with the liquid crystal sample mimics a false relaxation mode (ITO effect) around 1 MHz [3].

The following expression was fitted to the dielectric data:

$$\varepsilon^*(\omega) = \varepsilon(\infty) + \sum_j \frac{\Delta\varepsilon_j}{1 + \left(\mathrm{i}\frac{f}{f_{\mathrm{R}_j}}\right)^{\beta_j}} + \frac{1}{(\mathrm{i}\omega\tau_\mathrm{c})^\gamma} \qquad (1)$$

where $\Delta\varepsilon_j$, f_{R_j} and β_j are the dielectric amplitude, relaxation frequency and dispersion parameter of the j-th mode, respectively. The third term in expression (1) accounts for ionic conductivity, γ expressing the dispersion of 'conduction times' [4]. The helical pitch was measured by a diffraction method.

*Author for correspondence; e-mail: rachaves@fc.up.pt

Liquid Crystals ISSN 0267-8292 print/ISSN 1366-5855 online © 2001 Taylor & Francis Ltd
http://www.tandf.co.uk/journals
DOI: 10.1080/02678290110086532

3. Results and discussion

After cooling the sample from the isotropic phase and applying the electric field to ensure good alignment, the sample was heated back into the SmA* phase and the dielectric constant of 10FH was measured at 100 Hz, on cooling and heating. The values of the dielectric constant obtained during the first cooling run are about four times higher than those obtained on heating. This different cooling–heating behaviour was observed in all the dielectric measurements performed on three different 25 μm thick samples, for successive cooling/heating runs at different rates ($0.1 \Rightarrow 2$ K/min).

Figure 1 shows the real part of the dielectric constant, obtained during cooling and heating runs. After cooling the sample from the SmA* phase to the SmC^*_A phase and reheating it to the SmA* phase, the cooling/heating cycle was repeated several times. The values of the dielectric constant obtained during the second cooling run are lower than those obtained during the first cooling run, as shown in figure 1. The curve obtained during the third cooling run already resembles the curve obtained on heating, which is stable over several cooling/heating cycles (therefore, only one heating curve is presented in figure 1).

The compound 10FH shows visible disclination lines in a limited temperature interval that includes the lower temperature region of the SmC* phase and the ferrielectric region: specifically from 103 to 108°C on heating and from 106 to 101.7°C on cooling. An a.c. electric field ($1\ V\ \mu m^{-1}$, 10 Hz), was applied to the sample, for about 5 min during the third heating run, just below the temperature where disclination lines cease to be seen (≈ 107°C). The field was strong enough to obtain a saturated hysteresis loop. Figure 2 shows the result obtained from this experiment. After applying the electric field, the value of the dielectric constant increased and remained high. The sample was heated to the SmA* phase and then cooled again. During this fourth cooling, the values of the dielectric constant follow closely the curve obtained during the first cooling run.

The values of the dielectric constant measured in the SmC* phase at 100 Hz reflect mostly the contribution of the Goldstone mode. Figure 3 shows the real and imaginary parts of the dielectric constant, as a function of the frequency, obtained in the high temperature SmC* phase at ≈ 110°C on cooling and on heating. On cooling, the dielectric amplitude of the Goldstone mode is ≈ 170 and its relaxation frequency is ≈ 2 kHz, while on heating $\Delta\varepsilon_G \approx 50$ and $f_{R_G} \approx 4$ kHz (see figure 3).

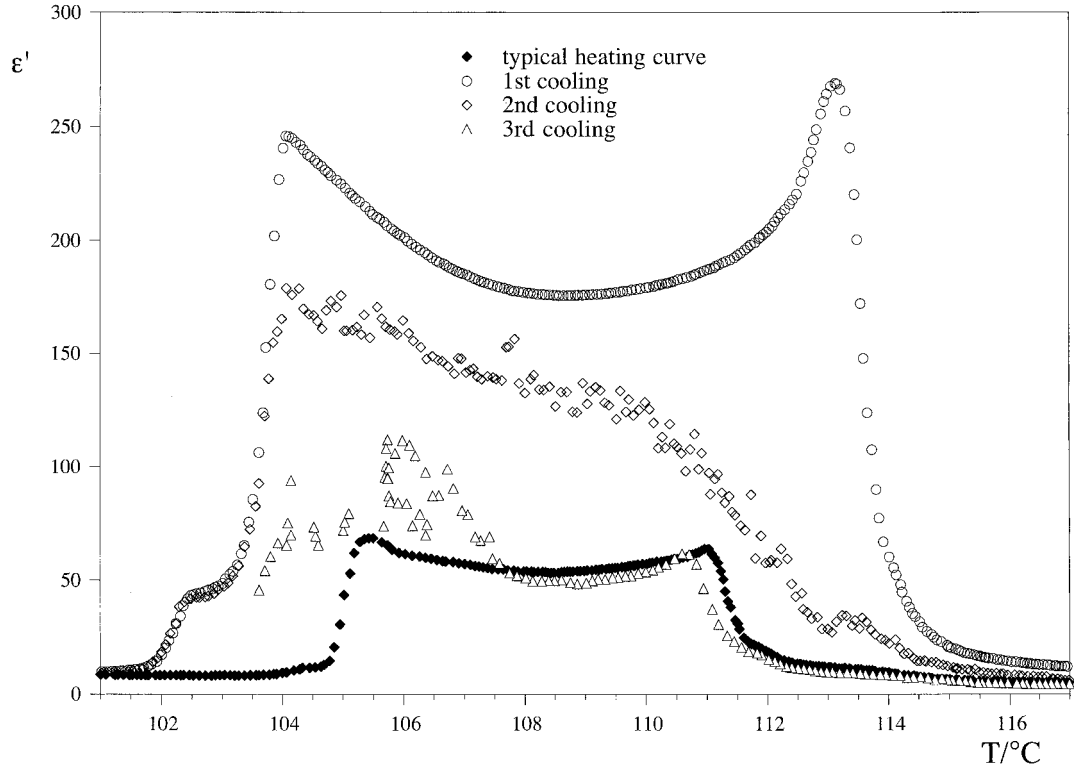

Figure 1. Real part of the dielectric constant, obtained at 100 Hz for 10FH, on several cooling runs and on a typical heating run.

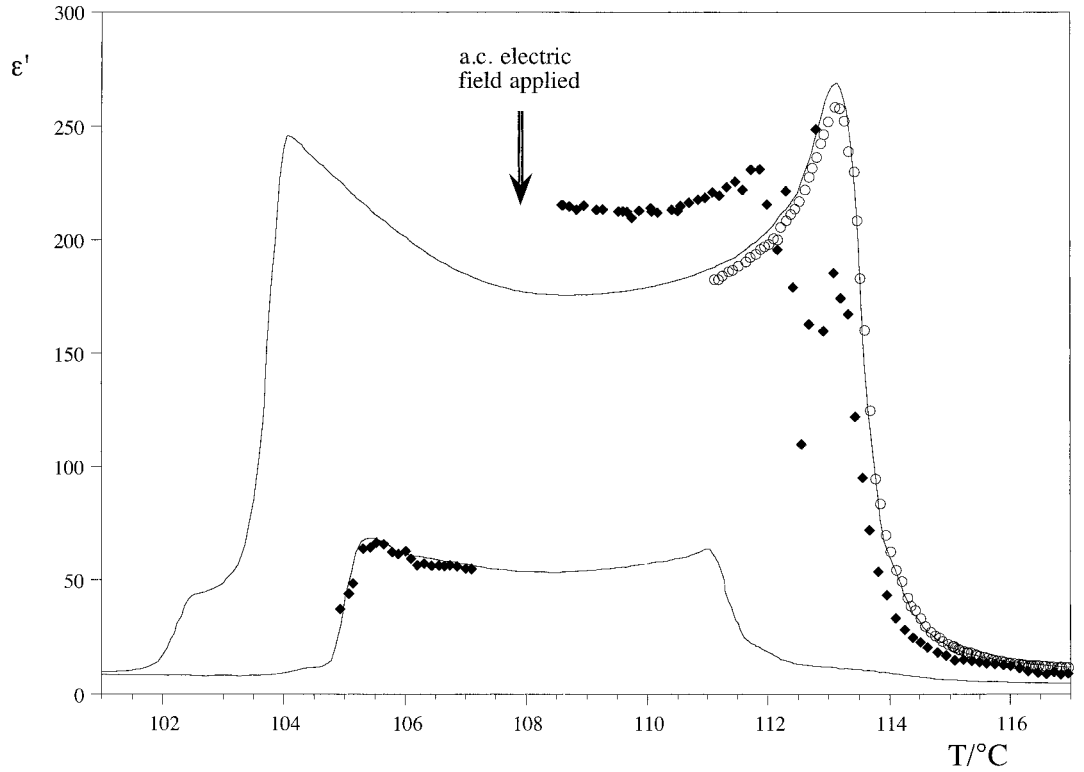

Figure 2. The third heating run (full diamonds) was interrupted and a strong a.c. electric field (1 V μm^{-1}, 10 Hz) was applied to the sample. The value of the dielectric constant increased and remained high. The fourth cooling run (open circles) follows the curve obtained during the first cooling. Both the typical heating curve and the first cooling run are presented here again (as full lines) for comparison.

The behaviour of the Goldstone mode in the SmC* phase is usually described well by the equations [5]:

$$\Delta\varepsilon_G = \frac{1}{4\pi\varepsilon_0}\frac{p^2}{2\pi K}\left(\frac{\mathbf{P}_0}{\theta_0}\right)^2$$

$$f_{R_G} = \frac{2\pi K}{p^2\gamma} \qquad (2)$$

where p is the helical pitch, and $\Delta\varepsilon_G$ and f_{R_G} are the dielectric amplitude and the relaxation frequency of the Goldstone mode, respectively. $\mathbf{P}_0$ and θ_0 are the spontaneous polarization and tilt angle, respectively, K is an elastic constant and γ a viscosity coefficient.

Assuming that K and γ do not change significantly with temperature, the equations (2) may suggest that the different dielectric contribution of the Goldstone mode on cooling and heating is due to a thermal hysteresis of the helical pitch, p. Nevertheless, such a hypothesis is not supported by a direct measurement of the helical pitch using the diffraction method. Within experimental error, the pitch measured on cooling in the SmC* phase, when the dielectric constant was high, was the same as the helical pitch obtained on heating for the same temperature, when the dielectric constant was lower. At $\approx$ 106–107°C, we obtained $p = 2.5 \pm 0.4\,\mu$m both on cooling and heating and before and after applying the electric field, for $\varepsilon'(100\,\text{Hz}) \approx 200$ and for $\varepsilon'(100\,\text{Hz}) \approx 50$. Therefore, it is clear that the different behaviour of the Goldstone mode, on cooling and on heating, is *not* related to a different value of the helical pitch.

A careful comparison of the $\varepsilon''(f)$ curves shown in figure 3 (*a*), for heating and cooling runs, reveals some interesting aspects that may lead to an interpretation of the anomalous thermal hysteresis observed for this compound. Both curves show that there are two different mechanisms contributing to $\varepsilon''(f)$: a relaxation process at higher frequencies and a second mechanism at lower frequency that is related to some conductivity process; third term of equation (1). The contribution of the relaxation process is clearly much larger on cooling than it is on heating, while the conductivity mechanism has a more important contribution on heating than on cooling. This behaviour indicates that the distribution and mobility of electric charges (ionic impurities, charged defects, etc.) in the sample are different on cooling and on heating runs. It can be inferred that the distribution of electric charges, near the surfaces or around structural defects, at a given temperature, depends on the 'history' of the sample.

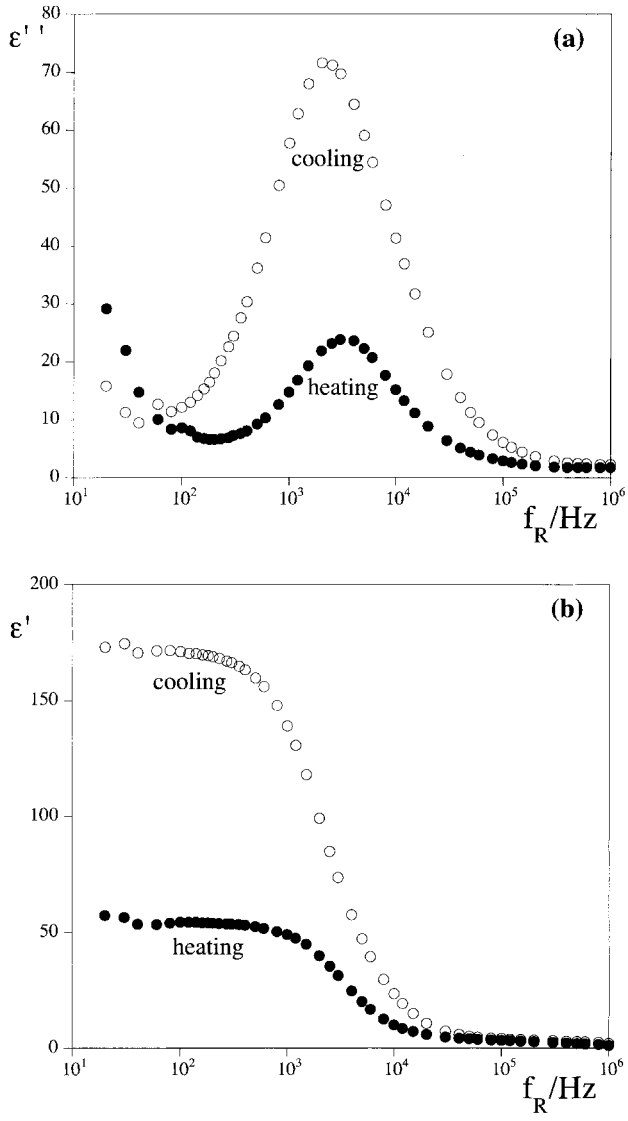

Figure 3. Imaginary (*a*) and real (*b*) parts of the dielectric constant, as a function of the frequency, obtained in the high temperature SmC* phase (≈ 110°C) on cooling and on heating.

The evidence presented in figure 3 for a different distribution of electric charges on cooling and heating runs leads us to suggest the following as an interpretation for the unusual behaviour of 10FH.

(1) When the sample is cooled from the isotropic phase, some of the existing electric charges will be fixed at defects or polarizing centres in the molecule, and consequently a certain distribution of charges (denoted type I) will occur in the sample. These trapped charges correspond to a stable pattern at high temperatures, when the sample is in the SmA* phase.

(2) The type I distribution of charges seems to remain stable in the high temperature range of the SmC* phase. In this temperature region, the helical pitch is large (2.5–3 μm), therefore the absence of visible disclination lines indicates a structure with π-disclinations at the surfaces, for which $\nabla \mathbf{P} = 0$ [6]. This type I distribution of charges becomes metastable as the temperature is lowered.

(3) At low temperatures, another distribution of charges (denoted type II) occurs, which is different from the one that was stable at high temperatures. Such a change may be due to several reasons. The structures of the low temperature SmC^*_{FI} and SmC^*_A phases are very different from those of the SmC* and SmA* phases. Furthermore, in the low temperature range of the SmC* phase, pairs of π-disclinations transform into 2π-disclinations, which remain throughout the ferrielectric region. 2π-disclinations are charged defects with $\nabla \mathbf{P} \neq 0$, therefore we may expect them to interfere with the local electric field and to influence the distribution of electric charges in the sample, by attracting charges of the opposite sign.

(4) The dielectric behaviour observed during the first cooling run is related to a type I distribution of charges which, although metastable at low temperatures, remains throughout the cooling run. Then a type II distribution is formed, determining the dielectric behaviour observed on heating. The type II distribution is metastable at high temperatures.

(5) When heated back to the SmA* phase, the system has some tendency to return to its original type I distribution of charges. The time needed for such a relaxation process to take place depends on the potential barrier that needs to be overcome. If this time is long there may be a memory effect, as observed in 10FH. The second cooling curve of figure 1 suggests that the type I distribution was not fully restored in the SmA* phase, leaving the system in a metastable intermediate state. As expected, the memory effect grows more pronounced as the cooling/heating cycle is repeated, so that the third cooling curve is very similar to the heating curve.

Both the compounds 11FH and 11HH studied in [1] and the two tolane derivatives in [6] show SmC^*_A and SmC^*_{FI} phases. All these compounds present visible disclination lines (2π-disclinations) only in the low temperature region of the SmC* phase and in the SmC^*_{FI} phase, but these compounds do not exhibit this thermal hysteresis. In fact, the behaviour shown by compound 10FH seems to be rather unusual, although a similar

anomalous thermal hysteresis was also observed for the compound C11 [7]. This leads us to believe that several factors may prevent the change from one distribution of electric charges to another, or reduce its effect. The mobility and quantity of ionic charges, the values of the viscosity coefficients and of the spontaneous polarization are probably critical parameters.

The process by which a different charge distribution may have such a strong influence on the characteristics of the Goldstone mode is not completely understood. It is well known [3] that this relaxation process is very sensitive to an applied d.c. electric field, so it is reasonable to suppose that a change in the local field (such as an internal bias field created by a charge distribution near the surfaces) may also influence the behaviour of the Goldstone mode.

This hypothesis of two different distributions of charges, one stable at high temperatures the other stable at low temperatures, remaining throughout cooling or heating runs, respectively, is also supported by the detailed study of the relaxation processes of 10FH. The dielectric relaxation results obtained for 10FH are summarized in figures 4, 5 and 6.

The behaviour of the ferrielectric mode (FIM) has been discussed [1]: its relaxation frequency is higher on heating than on cooling, but such a result was also found for 11FH and 11HH [1], therefore it is probably not related to the anomalous thermal hysteresis of 10FH. In this work we are concerned mainly with the soft mode, the Goldstone mode and the SLM, all of which show different behaviour on cooling and heating that may be related to a different distribution of electric charges in the sample for these runs.

Figure 6 shows that the dispersion parameter of the soft mode is higher on heating than on cooling. The same is true for the dispersion parameter of the Goldstone mode (see figure 6). The value of this parameter reflects the dispersion of the relaxation times.

Figure 5 shows that the dielectric contribution of the Goldstone mode decreases suddenly at $\approx 111°C$ on heating runs, while its relaxation frequency increases (see figure 4). This behaviour of the Goldstone mode suggests that a sudden decrease of the helical pitch occurs at $\approx 111°C$ during the heating run. A sudden decrease of the helical pitch, in the high temperature part of the SmC* phase, has already been observed for 11FH, both

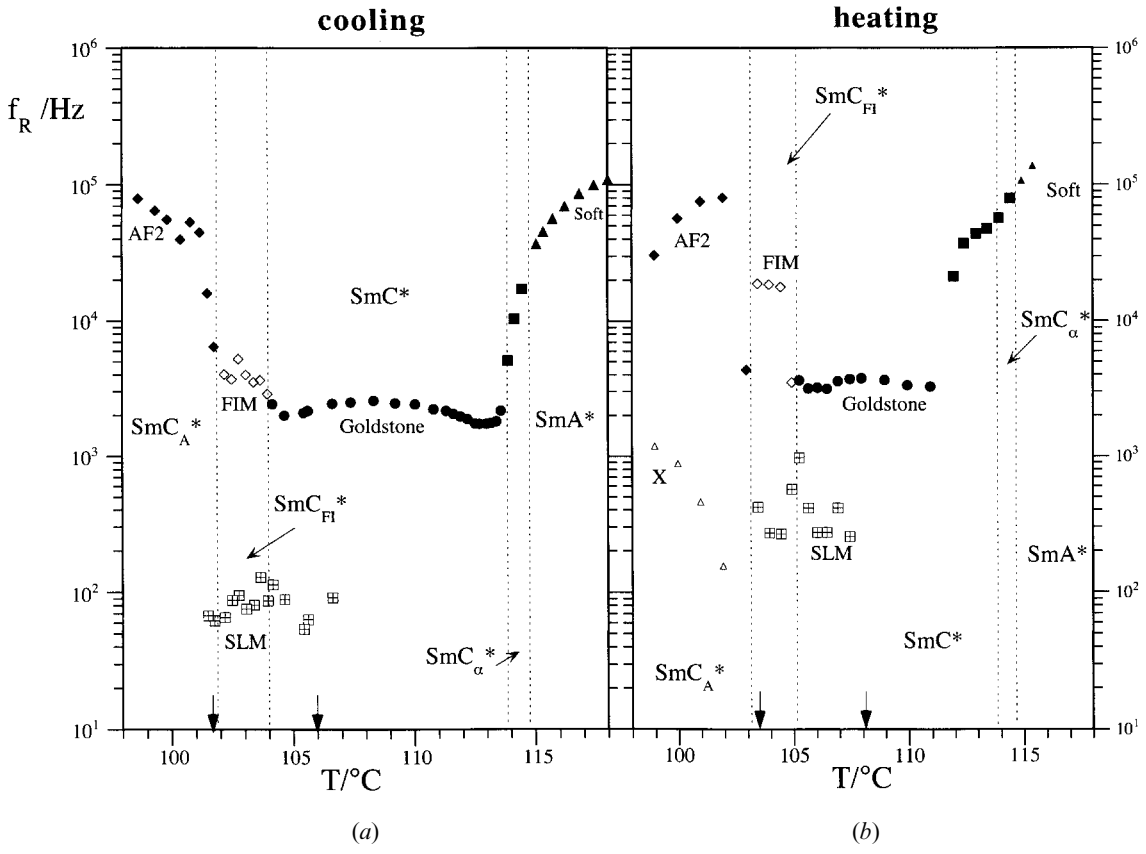

Figure 4. Relaxation frequencies of the modes observed for 10FH on cooling (*a*) and on heating (*b*). The arrows indicate the temperature range where disclination lines are observed without bias field.

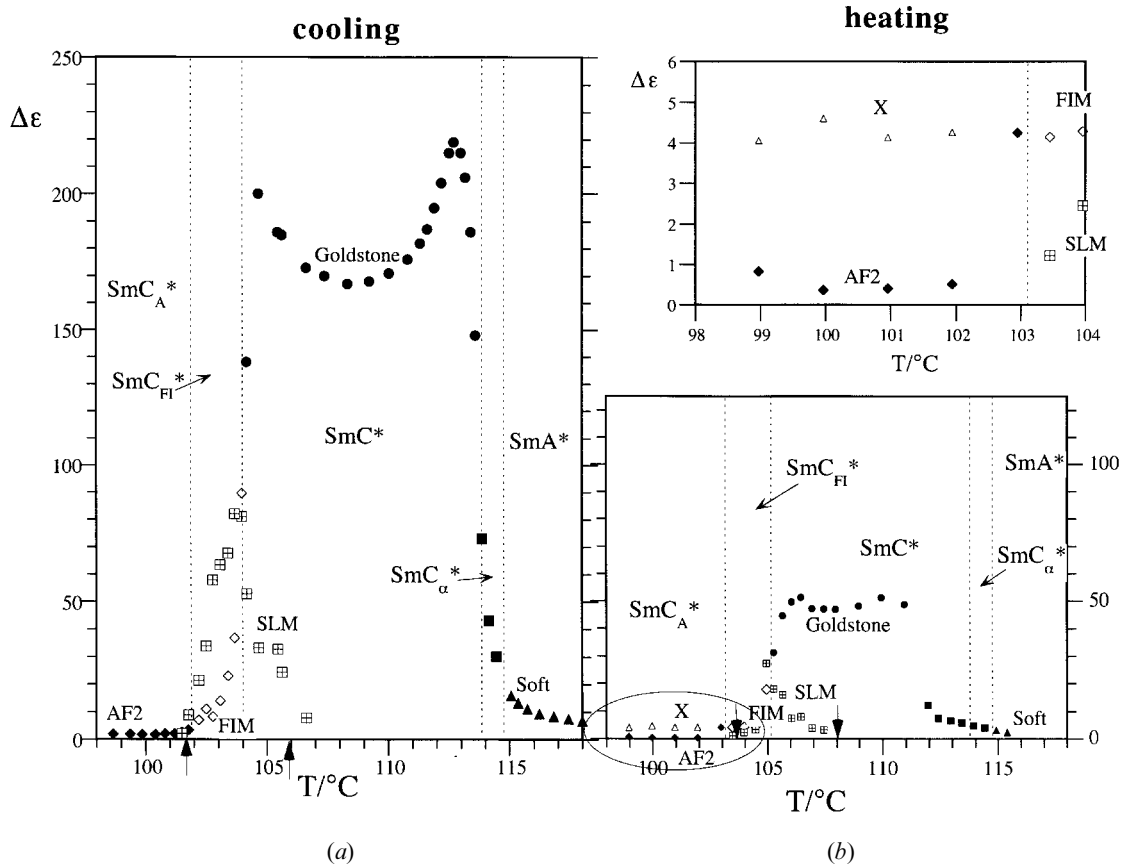

(*a*) (*b*)

Figure 5. Dielectric amplitudes of the modes observed for 10FH on cooling (*a*) and on heating (*b*).

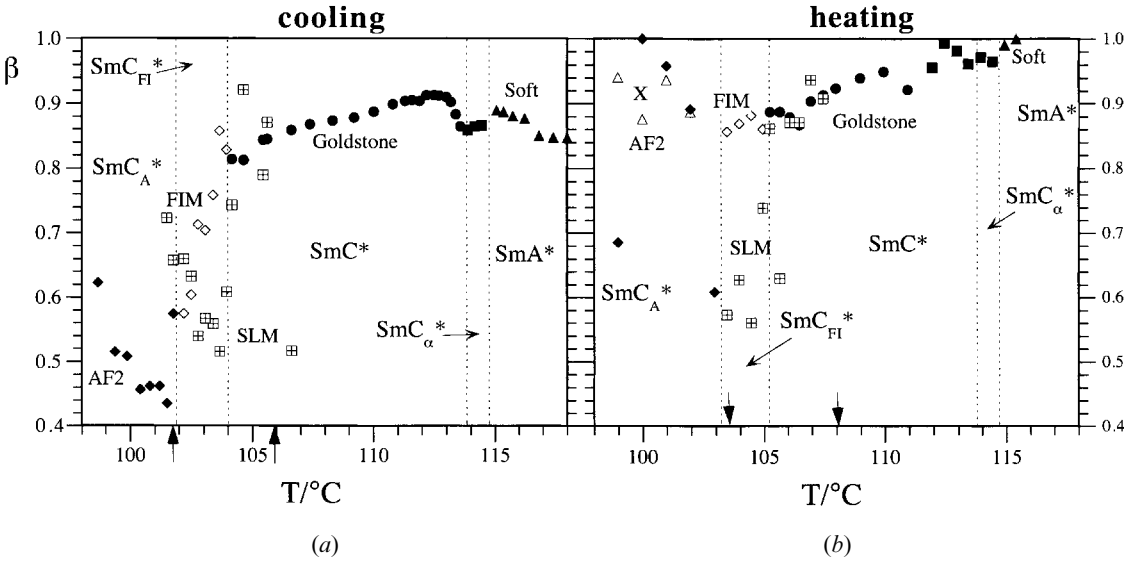

(*a*) (*b*)

Figure 6. Dispersion parameters of the modes observed for 10FH on cooling (*a*) and on heating (*b*).

on cooling and on heating [1]. It was interpreted as being related to the surface alignment conditions and the presence of π-disclinations. According to Pavel *et al.*, the interaction between π-disclinations of the same sign decreases the elastic energy [6]. For 10FH, this decrease of the helical pitch only takes place when the sample is in state II, during heating runs or after several cooling/heating cycles (see figure 1).

The SLM (surface layer mode) is detected in the lower temperature region of the SmC* phase and in the SmC^*_{FI} phase, whenever disclination lines are observed by polarizing microscopy. In our previous work, the SLM has been interpreted as the movement of 2π-disclinations [1], following Bourny *et al.* [8]. As 2π-disclinations are charged defects and can attract ionic charges during the slow cooling and heating processes, it is reasonable to expect the behaviour of the SLM to be strongly influenced by a change in the charge distribution of the sample. The response of the 2π-disclinations to the electric field will certainly be different from the response of 2π-disclinations with surrounding ionic charges.

As can be seen in figures 4 and 5, the relaxation frequency of the SLM is larger on heating runs than on cooling runs, while its dielectric contribution is smaller on heating runs than on cooling runs. This behaviour of the dielectric contribution of the SLM is particularly significant, as for both 11FH and 11HH, the dielectric amplitude of the SLM was observed to be higher on heating runs, corresponding to a greater density of visible disclination lines [1]. For 10FH although a greater number of lines is observed on heating, the maximum value of the dielectric amplitude attained on heating (≈ 30) is about a third of the maximum value of $\Delta\varepsilon_{SLM}$ on cooling (≈ 90), as can be seen in figure 5.

Finally, it is interesting to note the presence of the unidentified X-mode in figures 4 and 5. This mode was detected in the SmC^*_A phase of 10FH, but only on heating. Mode X could be related to the movement of ionic charges and other changes that take place in the sample, as it evolves from a type I to a type II distribution of charges.

4. Conclusions

The comparison of the $\varepsilon''(f)$ curves obtained on heating and cooling runs lead us to interpret the anomalous thermal hysteresis shown by the compound 10FH as being related to two different charge distributions in the sample. The type I distribution is stable at high temperatures and is largely related to the behaviour observed on cooling runs. The type II distribution of charges is stable only at low temperatures and is largely responsible for the dielectric behaviour observed on heating runs. The type II and type I distributions of charges appear to be related to the presence of 2π-disclinations and π-disclinations, respectively, although these defects are not the only factors determining the thermal hysteresis observed. Such an interpretation of the thermal hysteresis also explains successfully both the observed memory effect and the dielectric relaxation behaviour of 10FH.

The authors are grateful to Dr M. Glogarová for helpful discussions and to Albano Costa for his technical assistance. This work was supported by the project PRAXIS XXI/3/3.1/MMA/1769/95. S. Sarmento and F. Pinto thank project Praxis XXI for the grants BD/9545/96 and BIC J/4688/96.

References

[1] Sarmento, S., Simeão Carvalho, P., Chaves, M. R., Pinto, F., and Nguyen, H. T., 2001, *Liq. Cryst*., **28,** 673.
[2] Faye, V., Rouillon, J. C., Destrade, C., and Nguyen, H. T., 1995, *Liq. Cryst*., **19,** 47.
[3] Gouda, F., Skarp, K., and Lagerwall, S. T., 1991, *Ferroelectrics*, **113,** 165.
[4] Fukui, M., Orihara, H., Suzuki, A., Ishibashi, Y., Yamada, Y., Yamamoto, N., Mori, K., Nakamura, K., Suzuki, Y., and Kawamura, I., 1990, *Jpn. J. appl. Phys*., **29**, L329.
[5] Carlsson, T., Žeckš, B., Filipič, C., and Levstik, A., 1990, *Phys. Rev. A*, **42,** 877.
[6] Pavel, J., Gisse, P., Nguyen, H. T., and Martinot-Lagarde, P., 1995, *J. Physique II (Fr)*, **5,** 355.
[7] Simeão Carvalho, P., Glogarovà, M., Chaves, M. R., Nguyen, H. T., Destrade, C., Rouillon, J. C., Sarmento, S., and Ribeiro, M. J., 1996, *Liq. Cryst*., **21,** 511.
[8] Bourny, V., Pavel, J., Gisse, P., and Nguyen, H. T., 2000, *Ferroelectrics*, **241,** 247.